Cellular Physiology and Biochemistry

Cell Physiol Biochem 2018;51:1207-1220
DOI: 10.1159/000495498
Published online: 24 November 2018
Accepted: 16 November 2018

Original Paper

Pro-Angiogenic Activity of Monocytic-Type Myeloid-Derived Suppressor Cells from Balb/C Mice Infected with Echinococcus Granulosus and the Regulatory Role of miRNAs

Jian-hai Yin Cong-shan Liu Ai-ping Yu Jia-qing Yao Yu-juan Shen Jian-ping Cao

National Institute of Parasitic Diseases, Chinese Center for Disease Control and Prevention, Key Laboratory of Parasite and Vector Biology, MOH, National Center for International Research on Tropical Diseases, China, WHO Collaborating Center for Tropical Diseases, Shanghai, China

Key Words
MicroRNA • Monocytic-type myeloid-derived suppressor cells • Angiogenesis • Echinococcus granulosus

Abstract
Background/Aims: This study aims to predict the pro-angiogenic functions of monocytic-type myeloid-derived suppressor cells (M-MDSCs) derived from mice infected with *Echinococcus granulosus*. ***Methods:*** M-MDSCs were collected from Balb/c mice infected with *E. granulosus* and normal mice (control) and cultured *in vitro*. Human umbilical vein endothelial cells (HUVECs) were stimulated with the cell supernatant, and angiogenesis was investigated and analysed by the Angiogenesis module of the software NIH Image J. RNA was extracted from fresh isolated M-MDSCs and analysed with miRNA microarray; differentially expressed miRNAs and their potential functions were analysed through several bioinformatics tools. Finally, quantitative PCR was used to confirm the results of microarray analysis. ***Results:*** M-MDSCs from mice infected with *E. granulosus* could promote the formation of tubes from HUVECs *in vitro*. Moreover, vascular endothelial growth factor (VEGF) showed significantly high expression, whereas soluble fms-like tyrosine kinase-1 (sFlt-1) showed low expression at the transcriptional level in M-MDSCs from mice infected with *E. granulosus*. Microarray analysis of miRNAs showed that 28 miRNAs were differentially expressed in M-MDSCs from the two experimental mice groups, and 272 target genes were predicted using the microRNA databases TargetScan, PITA and microRNAorg. These target genes were mainly involved in the biological processes of intracellular protein transport, protein targeting to the lysosome and

J. Yin and C. Liu contributed equally to this work.

Jian-ping Cao
and Yu-juan Shen

National Institute of Parasitic Diseases, Chinese Center for Disease Control and Prevention, 207 Rui Jin 2nd Road, Shanghai 200025 (China)
Tel. +86-21-64723472, E-Mail caojp@yahoo.com; amyshyj12@163.com

protein transport, and mainly located in the cytoplasm, neuronal cell body and membrane. Moreover, they were mainly involved in the molecular functions of protein binding, metal ion binding and SH3 domain binding. Further, the differentially expressed miRNAs were mainly enriched in the endocytosis, Wnt and axon guidance pathways, as well as the MAPK, focal adhesion, PI3K-Akt, cAMP, mTOR and TGF-β signalling pathways, which are linked to immunoregulation and angiogenesis based on the results of bioinformatics analysis with DIANA-miRPath 3.0. In addition, the expression of eight miRNAs was randomly verified by quantitative PCR independently in three mice infected with *E. granulosus* and three normal mice. ***Conclusion:*** M-MDSCs have a potential angiogenic role during *E. granulosus* infection, and miRNAs may play a role in the immune response and angiogenesis functions of M-MDSCs through regulation of the identified signalling pathways.

Introduction

Cystic echinococcosis is an important zoonotic disease caused mainly by cystic growth of the metacestode of *Echinococcus granulosus*. The molecular mechanisms underlying its development and pathogenesis are still unclear [1-3], although it has been reported that this parasite can successfully escape host immune responses, and a number of immunoregulatory mechanisms related to macrophages and dendritic cells as well as regulatory T cells are potentially involved [2]. In our previous studies, we found that hydatid cysts of *E. granulosus* could promote the formation of tubes from human umbilical vein endothelial cells (HUVECs) *in vitro* [4], and that myeloid-derived suppressor cells (MDSCs) were significantly enriched in the spleen and peripheral blood of Balb/c mice infected with *E. granulosus* and played an immunosuppressive role [5]. The *in vitro* results are supported by other studies which have shown that angiogenesis is critical for parasites to acquire the nutrients necessary for growth, maturity and breeding after infection [6]. Moreover, MDSCs have been reported to be enriched in the host of parasitic infections and to play an important regulatory role in the interaction between parasitic pathogens and host clearance of parasites [7]. MDSCs, which are a group of heterogeneous cells derived from myeloid progenitor cells and immature cells, are classified into polymorphonuclear-type MDSCs and monocytic-type MDSC (M-MDSCs) [8]. Under normal physiological conditions, M-MDSCs differentiate into mature dendritic cells and macrophages, but they exert strong immunosuppressive effects and perform other functions such as pro-angiogenic functions in tumours, autoimmune diseases, viruses, bacteria and parasitic infections [9-12]. In the context of parasitic infection, studies mostly focus on the immunosuppressive function of MDSCs [7], and whether they also have a pro-angiogenic effect remains to be clarified. Research on pro-angiogenic factors associated with MDSCs and their mechanisms in *E. granulosus* infection could have important implications for the prophylaxis and treatment of echinococcosis.

The proliferation, differentiation, chemotaxis and function of MDSCs are influenced by many factors. In particular, microRNAs (miRNAs) play an important role *via* the regulation of related signalling pathways. For example, miR-494 activates MDSCs by inducing MMP-2, MMP-13 and MMP-14 through inhibiting tyrosine phosphatase (PTEN) [13]; miR-155 and miR-21 activate STAT3, which then promotes the enrichment of MDSCs and stimulate their immunosuppressive function [14]; miR-9 regulates the differentiation and function of MDSCs by targeting regulation of the expression of Runt-related transcription factor 1 [15]; miR-200c promotes the production of MDSCs and enhances their inhibitory ability through the regulation of PTEN and FOG2 expression [16]. On the other hand, miRNAs also play an inhibitory role. For example, miR-146a and miR-223 block MDSC enrichment [17, 18], and miR-17-5 and miR-20a silence STAT3 and reduce ROS and H_2O_2 production [19]. miRNA microarray and other high-throughput technology can help to detect the miRNA expression profile of tissues or cells, and combined with bioinformatics analysis of differentially expressed miRNA, it has become an important means of screening miRNA and predicting the regulatory role of the target genes of mRNAs in tissues or cells. Thus, identifying the

miRNAs that are differentially expressed in *E. granulosus* infection could shed light on the pro-angiogenic mechanisms of MDSCs.

The present study is the first to use M-MDSCs from mice infected with *E. granulosus* and to investigate their pro-angiogenic role through mouse miRNA microarray combined with bioinformatics methods and *in vitro* HUVEC tube formation assays. This study provides novel comparative information to potentially define the functional significance of angiogenesis-associated M-MDSC miRNAs in the potential pathophysiology of echinococcosis associated with *E. granulosus*.

Materials and Methods

Parasites and animals

This study was carried out in strict accordance with the recommendations of the guide for the care and use of laboratory animals of the Ministry of Science and Technology, China. The protocol was approved by the Laboratory Animals Welfare and Ethics Committee of National Institute of Parasitic Diseases, Chinese Center for Disease Control and Prevention (Permit Number: IPD-2014-2).

Live protoscoleces from sheep liver hydatid cysts were rinsed 5–8 times with phosphate-buffered saline (PBS) containing penicillin G (500 U/ml) and streptomycin (500 U/ml), and around 2, 000 protoscoleces were injected intraperitoneally into each Balb/c mouse (age, 4 weeks) purchased from the SLAC Laboratory Animal Center (Shanghai, China) [20].

M-MDSC isolation and culture

Single cell suspensions were prepared from the murine spleens after 8 months of infection with *E. granulosus* protoscoleces and from normal murine spleens (control group), as published previously [5]. Then, M-MDSCs were collected according to the instructions of the mouse Myeloid-Derived Suppressor Cell Isolation Kit (Miltenyi Biotec, Germany), and the cells were incubated with the following anti-mouse antibodies: PE-Gr-1, FITC-CD11b, APC-Ly-6G and PerCP-Cy5.5-Ly-6C. M-MDSCs of >90% purity were obtained for the following experiments, and the purity was determined using flow cytometry. All the antibodies were purchased from eBioscience, an Affymetrix Company. M-MDSCs were seeded at a density of 10^6 cells/well in 24-well plates with RPMI-1640 (Gibco, USA) (containing 100 U/ml penicillin and 100 U/ml streptomycin), and incubated at 37°C in a 5% CO_2/95% air atmosphere. The supernatant was collected after 24 h through centrifugation at 2500 × g for 10 min.

HUVEC culture and tube formation assay

HUVECs were purchased from ScienCell Research Laboratories (USA), and cultured and maintained according to the manufacturer's instructions. Endothelial cell medium, bovine plasma fibronectin, Dulbecco's Phosphate Buffered Saline (DPBS) (Ca^{++} and Mg^{++} free), trypsin/EDTA solution and trypsin neutralization solution were also from ScienCell Research Laboratories, and T-75 flasks were from Corning (USA). All the following assays were conducted using low cell passage cells (3-5 passages).

The effect of M-MDSCs on HUVEC differentiation was examined by *in vitro* tube formation on the Matrigel matrix (BD Biosciences, USA). HUVECs that reached over 90% confluence were harvested and diluted to a density of 3 × 10^5 cells/ml using the RPMI-1640 medium (containing 100 U/ml penicillin and 100 U/ml streptomycin). Then, 100 μL of HUVEC suspension was mixed with 100 μL M-MDSC culture supernatant from the infection group or RPMI-1640 medium (containing 100 U/ml penicillin and 100 U/ml streptomycin) per well of 96-well plates and incubated at 37°C under 5% CO_2/95% air. The tube-like structures were investigated under an inverted microscope, and the number of nodes in three random fields per well was quantified using the angiogenesis module of the NIH Image J software [21, 22].

RNA extraction and microassay

Total RNA, which includes microRNA, was extracted from the M-MDSCs according to the protocol of the mirVana isolation kit (Applied Biosystems, USA), and purified with the RNeasy Mini Kit (Qiagen, Germany). The purity and concentration of the RNA were determined using OD260/280/230 readings with a NanoDrop ND-2000 spectrophotometer (Thermo Fisher Scientific, USA). The integrity of the RNA was

determined using the Agilent BioAnalyzer 2100 (Agilent Technologies, USA). Sample labelling, microarray hybridization, and washing were performed in accordance with the manufacturer's standard protocols. After washing, the microarrays were scanned using the Agilent Scanner G2505C (Agilent Technologies, USA). All microarray experiments were performed by Shanghai OE Biotech Co. Ltd., Shanghai, China.

Biostatistical analysis

The Feature Extraction software (version 10.7.1.1; Agilent Technologies, USA) was used to analyse array images to obtain raw data, which was normalized using the Quantile algorithm. Next, the Genespring software (version 13.1; Agilent Technologies, USA) was used for the following data analysis. Differentially expressed miRNAs were then identified based on fold changes in expression, and the P value was calculated using the t-test. The threshold for up- and downregulated genes was a fold change of ≥2 and a P value of ≤0.05.

The target genes of differentially expressed miRNAs were predicted using three online databases—TargetScan, PITA, and microRNAorg. Gene ontology (GO) analysis and Kyoto Encyclopedia of Genes and Genomes (KEGG) pathway analysis were used to determine the potential biological roles of the target genes. Hierarchical clustering was performed to identify the miRNA expression patterns of the samples. To investigate whether coexpression of the deregulated miRNAs could affect angiogenic signalling in M-MDSCs from *E. granulosus*-infected mice by targeting angiogenic factors, the web-based computational tool DIANA-miRPath (version 3.0) [23] was used.

Detection of VEGF and sFlt in M-MDSCs by quantitative PCR

MDSCs secrete various pro-angiogenic factors including vascular endothelial growth factor (VEGF), which is the strongest stimulator of endothelial cell proliferation and activation and plays a central role in angiogenesis [24-26]. In contrast, soluble fms-like tyrosine kinase-1 (sFlt-1) is a tyrosine kinase protein that disables proteins that cause blood vessel growth [27-29]. In the present study, we investigated the expression of VEGF and sFlt-1 in M-MDSCs from *E. granulosus*-infected mice and normal controls at the transcriptional level, in order to indirectly evaluate the angiogenic role of M-MDSCs. Total RNA from M-MDSCs was extracted as above, and a total of 1 μg RNA was used as template for first-strand DNA synthesis (Bio-Rad, USA). The primer sequences specific to mouse VEGF were 5'-GAGTACCCCGACGAGATAGA-3' (forward) and 5'-GGCTTTGGTGAGGTTTGAT-3' (reverse); mouse sFlt-1, 5'-GGGAAGACATCCTTCGGAAGA-3' (forward) and 5'-TCCGAGAGAAAATGGCCTTTT-3' (reverse); mouse GAPDH (internal control), 5'-GCCTTCCGTGTTCCTACC-3' (forward) and 5'-GCCTGCTTCACCACCTTC-3' (reverse). The cycling protocol was as follows: 95°C for 30 s, followed by 40 cycles of 95°C for 5 s, 60°C for 10 s, and 72°C for 30 s. A melting curve was generated by cooling the products to 65°C and then heating to 95°C at a rate of 0.1°C/s while simultaneously measuring fluorescence.

Validation of microarray data by qPCR analysis

Eight differentially expressed miRNAs were randomly selected and validated with M-MDSCs from an independent set of three mice after 8 months of infection with *E. granulosus* and three normal mice, using qPCR with SYBR Green PCR Master Mix (Toyobo, Japan) and the following specifically designed primers, using the C1000 Touch Thermal Cycler (Bio-Rad, USA): mmu-miR-29a-3p, 5'-TAGCACCATCTGAAATCGGTTA-3'; mmu-miR-150-5p, 5'-TCTCCCAACCCTTGTACCAGTG-3'; mmu-miR-151-5p, 5'-TCGAGGAGCTCACAGTCTAGT-3'; mmu-miR-17-3p, 5'-ACTGCAGTGAGGGCACTTGTAG-3'; mmu-miR-181a-5p,5'-AACATTCAACGCTGTCGGTGAGT-3';mmu-miR-30b-5p,5'-TGTAAACATCCTACACTCAGCT-3';mmu-miR-30c-5p, 5'-TGTAAACATCCTACACTCTCAGC-3'; mmu-miR-3535, 5'-TGGATATGATGACTGATTACCTGAGA-3'. U6 RNA was selected as a housekeeping miRNA for normalization of miRNA expression. Total RNA from the cells was reverse transcribed to cDNA according to the instructions of the Mir-X miRNA qRT-PCR SYBR kit (Takara, USA). Each 20 μL qPCR reaction mixture contained 10 μL of SYBR Green PCR Master Mix (Toyobo, Japan), 0.5 μL of a forward/reverse primer mixture, 2 μL of cDNA template, and 7 μL of nuclease-free H_2O (Promega, USA). The cycling protocol was the same as above.

Statistical analysis

Differences in HUVEC tube formation was determined with the t-test, based on observation of the nodes of the tube-like structures stimulated by M-MDSCs and RPMI-1640, using GraphPad Prism (version 5.0). Quantification of each mRNA and miRNA relative to the controls (GAPDH and U6) was performed using the $2^{-\Delta\Delta Ct}$ method. A P value of <0.05 was considered to indicate statistical significance. All assays were performed in triplicate.

Results

Evaluation of the in vitro pro-angiogenic role of M-MDSCs

HUVECs were stimulated with the supernatant of M-MDSCs and RPMI-1640; HUVEC tube formation was observed every 1 h, and the total number of nodes was calculated at 3 h. The results showed that the total number of nodes in the M-MDSC group (192 ± 34.5) was significantly higher than that in the RPMI-1640 group (143 ± 10.4) (P = 0.017) (Fig. 1). Moreover, analysis of the transcriptional expression of VEGF and sFlt-1 in M-MDSCs showed that the expression of VEGF was higher in *E. granulosus*-infected mice than in normal control mice (P < 0.001) and that the expression of sFlt-1 (P = 0.026) was downregulated (Fig. 2).

Differentially expressed miRNAs in M-MDSCs from mice infected with E. granulosus

Differentially expressed miRNAs in M-MDSCs were screened with the Agilent mouse miRNA microarray (8 × 60 K, ID: 070155). A total of 28 miRNAs were differentially expressed between *E. granulosus*-infected and uninfected Balb/c mice based on fold changes in their expression and significance, including two upregulated miRNAs (mmu-miR-7040-5p and mmu-miR-7042-5p) and 26 downregulated miRNAs (Fig. 3 & Table 1).

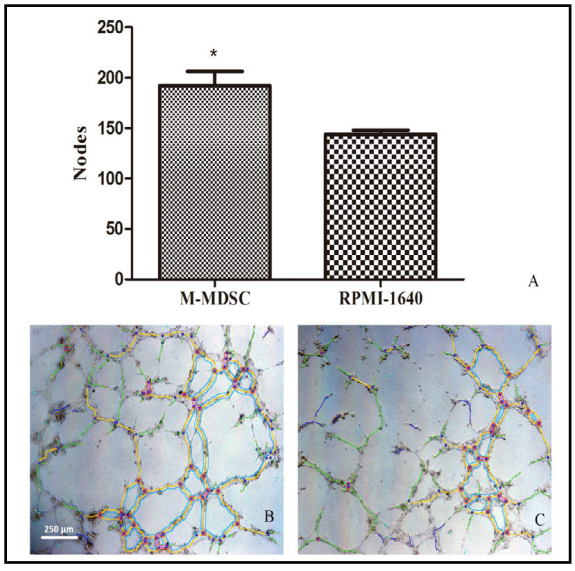

Fig. 1. M-MDSCs promote HUVEC tube formation in vitro. (a) Number of nodes on the tubes stimulated with the culture supernatant of M-MDSCs from E. granulosus-infected mice and RPMI-1640. (b) HUVEC tube formation stimulated with the culture supernatant of M-MDSCs from E. granulosus-infected mice. (c) HUVEC tube formation stimulated with RPMI-1640. *P<0.05 versus Control.

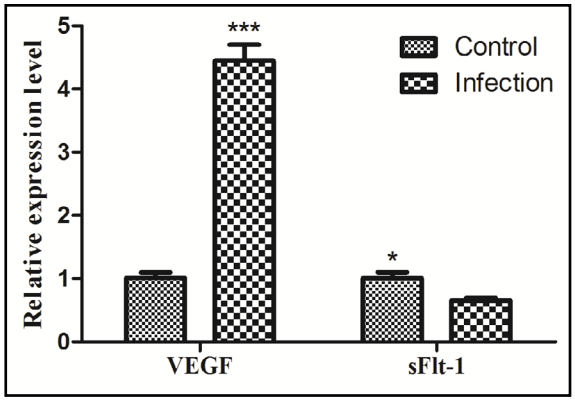

Fig. 2. Transcriptional expression of VEGF and sFlt-1 in M-MDSCs from infected and uninfected mice. ***P<0.001 versus Control; n = 3.

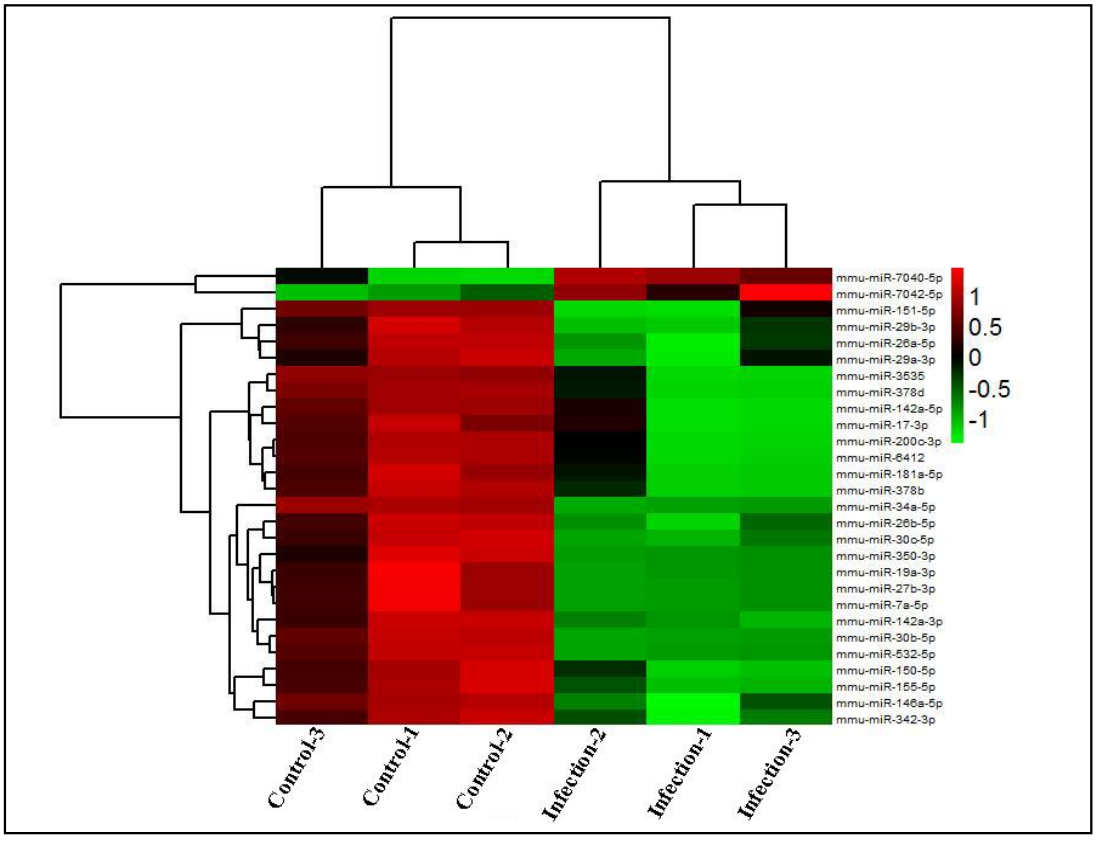

Fig. 3. Differentially expressed miRNAs in M-MDSCs from mice infected with E. granulosus. Heat map showing the details of 28 miRNAs in M-MDSCs differentially expressed in mice infected with E. granulosus and normal mice, n = 3.

Biological functions of the differentially expressed miRNAs

The target genes of the differentially expressed M-MDSC miRNAs following *E. granulosus* infection and their functions were predicted using GO analysis and KEGG pathway analysis. A total of 272 common target genes were identified using the TargetScan, PITA and microRNAorg databases (Fig. 4). Then, the top 20 enriched genes were classified according to GO functional annotations (Fig. 5). The findings revealed that some of the predicted target genes played potentially important biological functions in the host during *E. granulosus* infection. The GO-specific functions mainly included biological processes (e.g. intracellular protein transport, protein targeting to the lysosome and protein transport) (Fig. 5a), molecular functions (e.g. protein binding, metal ion binding and SH3 domain binding) (Fig. 5b), and cell components (e.g. cytoplasm, neuronal cell body and membrane) (Fig.

Table 1. Fold-changes and P-values of differentially expressed miRNAs in M-MDSCs from mice infected with E. granulosus (n = 3)

miRNA name	P	Fold change	Regulation
mmu-miR-142a-3p	0.003683	2.136092	down
mmu-miR-142a-5p	0.031297	55.82497	down
mmu-miR-146a-5p	0.004776	4.716855	down
mmu-miR-150-5p	0.011318	2.201012	down
mmu-miR-151-5p	0.025226	4.483565	down
mmu-miR-155-5p	0.004861	2.018359	down
mmu-miR-17-3p	0.039841	11.83214	down
mmu-miR-181a-5p	0.018907	11.87966	down
mmu-miR-19a-3p	0.005433	10.10234	down
mmu-miR-200c-3p	0.020941	9.242744	down
mmu-miR-26a-5p	0.012041	2.310433	down
mmu-miR-26b-5p	0.00446	2.655252	down
mmu-miR-27b-3p	0.004514	10.23533	down
mmu-miR-29a-3p	0.028465	2.642384	down
mmu-miR-29b-3p	0.013601	2.682152	down
mmu-miR-30b-5p	5.15E-04	48.26751	down
mmu-miR-30c-5p	0.003911	2.831918	down
mmu-miR-342-3p	0.00916	2.05773	down
mmu-miR-34a-5p	6.97E-07	9.956879	down
mmu-miR-350-3p	0.007105	12.66902	down
mmu-miR-3535	0.009708	10.55518	down
mmu-miR-378b	0.009754	19.82632	down
mmu-miR-378d	0.008849	37.37995	down
mmu-miR-532-5p	0.001059	8.209475	down
mmu-miR-6412	0.019074	9.782905	down
mmu-miR-7a-5p	0.003871	10.38286	down
mmu-miR-7040-5p	0.014211	2.129001	up
mmu-miR-7042-5p	0.012418	2.00102	up

5c). In addition, a total of 16 pathways (e.g. endocytosis, the Wnt signalling pathway and axon guidance) were predicted using KEGG pathway analysis (Fig. 6).

Angiogenesis-related pathway enrichment analysis

A total of 66 diverse signalling pathways associated with 26 deregulated miRNAs were identified through DIANA-miRPath (3.0) analysis (Table S1 - For all supplemental material see www.karger.com/10.1159/000495498), but no pathway associated with the two upregulated miRNAs was found. This study focused on six pathways involved in angiogenesis: MAPK, focal adhesion, PI3K-Akt, cAMP, mTOR, and TGF- signalling. Of the 26 deregulated miRNAs, 24 were associated with the MAPK signalling pathway *via* 108 diverse genes; 23 deregulated miRNAs were associated with the focal adhesion signalling pathway and PI3K-Akt signalling pathway *via* 89 and 131 diverse genes individually; 22 deregulated miRNAs were linked to the cAMP signalling pathway and mTOR signalling pathway *via* 83 and 32 diverse genes respectively; 21 deregulated miRNAs were associated with TGF-beta signalling pathways *via* 38 diverse genes (Table S2). Interestingly, 19 of the deregulated miRNAs were commonly associated with six of the above pathways (Fig. 7).

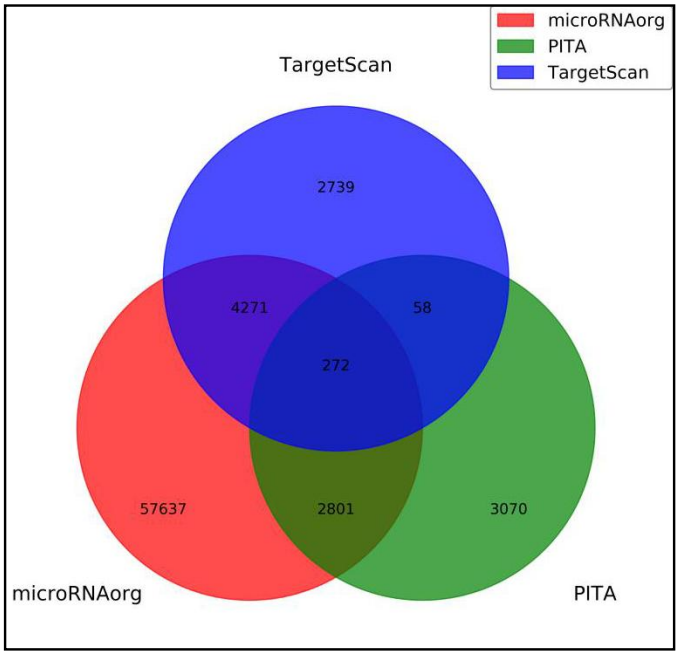

Fig. 4. Integrated analysis of the predicted target genes of differentially expressed miRNAs in M-MDSCs. Venn diagram showing the predicted target genes found in the databases TargetScan, PITA, and microRNAorg. A total of 272 of these genes were found in all three databases.

Validation of miRNA microarray data by qPCR analysis

qPCR analysis of eight differentially expressed miRNAs, which were randomly selected, and the housekeeping miRNA miR-U6 was performed to validate the results of microarray analysis. The expression patterns confirmed by qPCR were consistent with those of the microarray data, and provided further evidence that mmu-miR-29a-3p (P = 0.049), mmu-miR-150-5p (P = 0.002), mmu-miR-151-5p (P < 0.001), mmu-miR-17-3p (P = 0.009), mmu-miR-181a-5p (P <0.001), mmu-miR-30b-5p (P = 0.046), mmu-miR-30c-5p (P = 0.006), and mmu-miR-3535 (P = 0.001) were deregulated in M-MDSCs from *E. granulosus*-infected mice (Fig. 8).

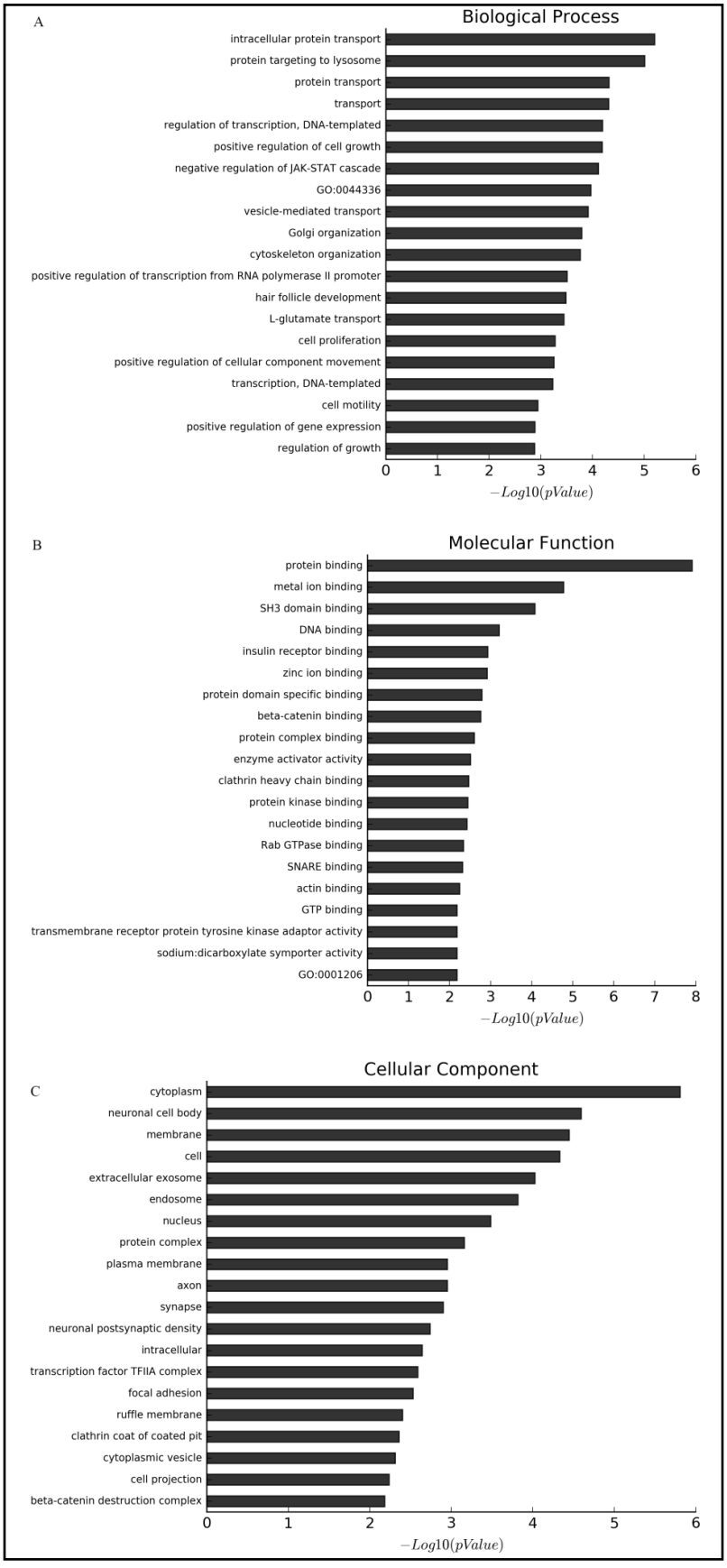

Fig. 5. GO analysis of the predicted target genes of differentially expressed miRNAs in M-MDSCs. According to the –Log10 (P value), the top 20 GO terms for biological process (A), molecular function (B) and cellular component (C) are shown.

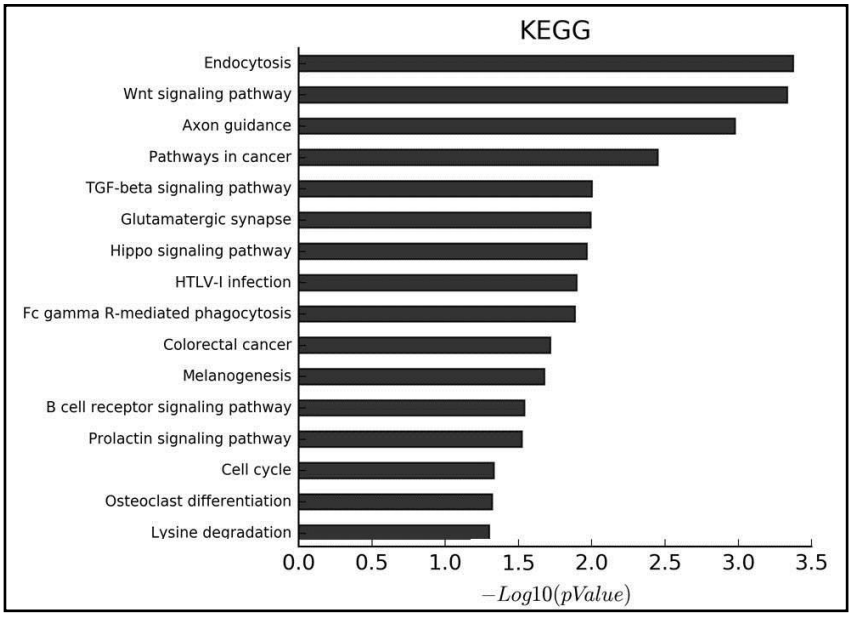

Fig. 6. KEGG enrichment analysis of the predicted genes of differentially expressed miRNAs in M-MDSCs. Pathways are ranked by $-\text{Log}_{10}$(P-value).

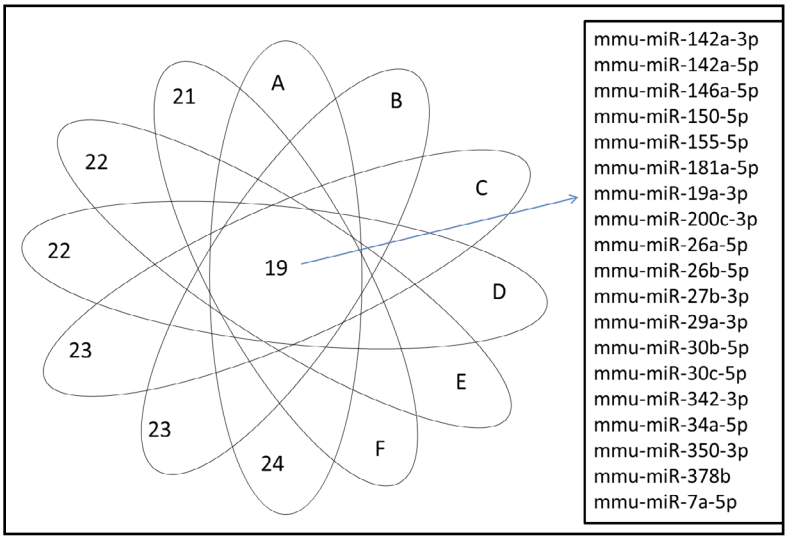

Fig. 7. Venn diagrams representing commonly deregulated miRNAs in six angiogenesis-related signalling pathways. A total of 19 deregulated miRNAs were shared by the six angiogenesis-related signalling pathways. A: MAPK signalling pathway, B: Focal adhesion pathway, C: PI3K/Akt signalling pathway, D: cAMP signalling pathway, E: mTOR signalling pathway, F: TGF-beta signalling pathway.

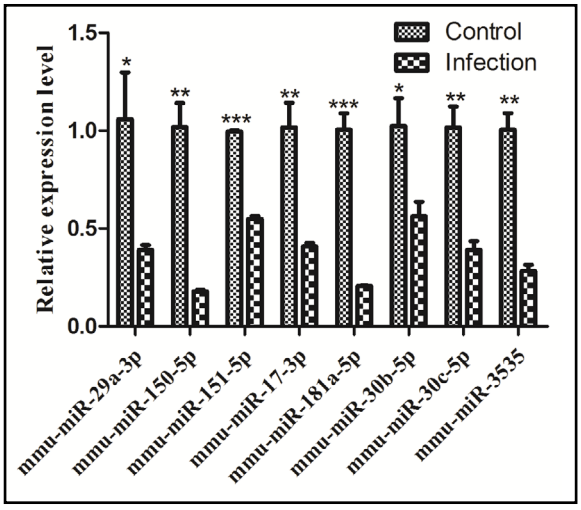

Fig. 8. Verification of miRNAs by qPCR. Eight differentially expressed miRNAs were randomly selected to validate the results of microarray analysis compared with the housekeeping miRNA miR-U6. *P<0.05 versus Control, **P<0.01 versus Control, ***P<0.001 versus Control; n = 3.

Discussion

The present study has, for the first time, elucidated the pro-angiogenic role of MDSCs in echinococcosis using miRNA microarray analysis. M-MDSCs from mice infected with *E. granulosus* were found to promote tube formation of HUVECs *in vitro*; moreover, high expression of VEGF and low sFlt-1 expression in M-MDSCs from *E. granulosus* indicated that this cell population has a pro-angiogenic role. Additionally, differentially expressed miRNAs in M-MDSCs were screened with the Agilent mouse miRNA microarray (8 × 60 K, ID: 070155), and the corresponding target genes and their potential functions provide support for further understanding the underlying mechanisms.

In the present study, six signalling pathways related to angiogenesis were identified based on GO and KEGG analysis of the dysregulated miRNAs. Of the identified pathways, the PI3K/AKT/mTOR signalling pathway and/or the MAPK signalling pathway can enhance the secretion of VEGF [30-32], which is the most important pro-angiogenic factor. However, the expression of different members of the VEGF family may depend on different pathways. For example, in head and neck squamous cell carcinomas, the expression of VEGF-A depends on the PI3K and MAPK signalling pathways, whereas the expression of VEFG-C depends on the MAPK signalling pathway [30, 31]. Moreover, the PI3K/AKT signalling pathway is also involved in regulation of the expression of NO and other angiogenic factors [32]. In particular, the PI3K pathway can regulate the expression of several transcription factors related to MDSC proliferation and survival and related genes [33]. The mTOR pathway can regulate the inflammatory response by affecting the NF Kappa B and STAT3 activity of myeloid cells, and participate in the regulation of the generation and differentiation of myeloid cells [34, 35]; moreover, it may play an important role in the generation of MDSCs. Another identified pathway in the present study was TGF-β signalling. TGF-β is a pleiotropic cytokine that is involved in the regulation of cell proliferation, growth and migration, and may serve as a positive or negative transcriptional regulator based on its target genes and intracellular environment. MDSCs are an important source of TGF-β [36], and TGF-β can modulate MDSC proliferation and function indirectly by inducing the expression of certain miRNAs [13]. Finally, the focal adhesion kinase pathway was also identified in the present study. It is also widely involved in cell migration, proliferation and invasion, and can promote the migration of endothelial cells and angiogenesis [37-39]. All these findings indicate that miRNAs play an important regulatory role in the signalling pathways that affect M-MDSC proliferation, expansion and function [40]. In this study, the target genes of the differentially expressed miRNAs were found to be enriched in these major signalling pathways involved in cellular immune regulation and regulation of angiogenesis. Thus, these signalling pathways may be involved in the pro-angiogenic mechanisms of MSDCs in echinococcosis.

Several differentially expressed miRNAs identified in this study have been found to be involved in the regulation of angiogenesis by different mechanisms in various studies. For example, upregulation of miR-150-5p can affect the activity and proliferation of endothelial cells (such as RF/6A) by binding to VEGF, and reduce the number of migratory cells and inhibit tube formation [41, 42]. Moreover, the expression of miR-17-3p, a member of the miR-17-92 cluster, is negatively correlated with the expression of VEGF [43]; miR-17-3p binds to the 21-bp domain of the UTR of the 3'end of Flk-1, resulting in rapid downregulation of Flk-1 and negative regulation of angiogenesis in HUVECs [44]. MMP-14 could be downregulated by post-transcriptional regulation through the combination of miR-181a-5p and an element in the UTR of the 3'-end of MMP-14, thereby effectively inhibiting tumour cell migration and tumour angiogenesis, and play a potential anti-metastatic role [45]. miR-26b-5p is a tumour suppressor miRNA that inhibits angiogenesis by downregulating the expression of factors, such as vascular endothelial cadherin and MMP-2, and could present a promising treatment target of hepatocellular carcinoma [46]. miR-142a-3p can directly inhibit vascular endothelial cadherin, and its overexpression can lead to the destruction of vascular integrity, vascular remodelling and pathological bleeding; moreover, abnormal vessels can be reconstructed when the function of miR-142a-3p is blocked [47]. MiR-34a-5p

could inhibit VEGFA expression and suppress endometrial-derived stem cell proliferation by targeting the UTR of the 3'-end of VEGFA [48]. MiR-26a/b have also been shown to have strong anticancer effects through regulation of different molecular targets associated with the extracellular matrix and cell cycle regulation during cancer development. For example, miR-26a-5p and miR-26b-5p could directly suppress cell aggressiveness by regulating procollagen-lysine, 2-oxoglutarate 5-dioxygenase 2 (PLOD2), which is associated with the stiffness of the extracellular matrix in bladder cancer [49]. Moreover, miR-26a/b could bind to the 3'-UTR of HGF mRNA at specific target sites, and their overexpression could repress the HGF-VEGF pathway and suppress tumour growth and angiogenesis in a xenograft mouse model [50]. Furthermore, miR-26a could bind to the 3'-UTR of PIK3C2α mRNA, resulting in downregulation of VEGFA expression, and inhibit angiogenesis via the PI3K C2α/Akt/HIF-1α/VEGFA pathway in hepatocellular carcinoma [51]. MiR-27b can also function as an angiogenesis inhibitor by targeting the VEGF-C/VEGFR2 axis [52]. Thus, these findings provide further proof of the regulatory role of the identified miRNAs in the pro-angiogenic functions of MSDCs and may even explain pro-angiogenic mechanisms in other parasitic diseases.

Conclusion

In summary, M-MDSCs not only have immunomodulatory function, but may also participate in angiogenesis during *E. granulosus* infection; moreover, miRNAs have a potential regulatory role in these two functions.

Acknowledgements

The authors would like to thank professor Jun-ying Ma at Qinghai Institute for Endemic Disease Prevention and Control for her help in collecting the parasite samples in Qinghai Province, China. This work was supported by the National Natural Science Foundation of China (No. 81702030 to JHY, Nos. 81772224 and 81371842 to YJS, No. 81772225 to JPC) and the Fourth Round of Three-Year Public Health Action Plan of Shanghai, China (No. 15GWZK0101 to JPC).

Disclosure Statement

The authors have no conflicts of interest to declare.

References

1 Kern P, Menezes da Silva A, Akhan O, Mullhaupt B, Vizcaychipi KA, Budke C, Vuitton DA: The echinococcoses: diagnosis, clinical management and burden of disease. Adv Parasitol 2017;96:259-369.
2 Gottstein B, Soboslay P, Ortona E, Wang J, Siracusano A, Vuitton D: Immunology of alveolar and cystic echinococcosis (AE and CE). Adv Parasitol 2017;96:1-54.
3 Deplazes P, Rinaldi L, Alvarez Rojas CA, Torgerson PR, Harandi MF, Romig T, Antolova D, Schurer JM, Lahmar S, Cringoli G, Magambo J, Thompson RC, Jenkins EJ: Global distribution of alveolar and cystic echinococcosis. Adv Parasitol 2017;95:315-493.
4 Yin J, Shen Y, Yu A, Cao J: *In vitro* pro-angiogenic activity of *Echinococcus granulosus* hydatid cysts from experimentally infected mice. Chin J Schi Contl 2017;29:320-323.
5 Pan W, Zhou HJ, Shen YJ, Wang Y, Xu YX, Hu Y, Jiang YY, Yuan ZY, Ugwu CE, Cao JP: Surveillance on the status of immune cells after *Echinnococcus granulosus* protoscoleces infection in Balb/c mice. PLoS ONE 2013;8:e59746.

6 Dennis RD, Schubert U, Bauer C: Angiogenesis and parasitic helminth-associated neovascularization. Parasitology 2011;138:426-439.
7 Van Ginderachter JA, Beschin A, De Baetselier P, Raes G: Myeloid-derived suppressor cells in parasitic infections. Eur J Immunol 2010;40:2976-2985.
8 Youn JI, Nagaraj S, Collazo M, Gabrilovich DI: Subsets of myeloid-derived suppressor cells in tumor-bearing mice. J Immunol 2008;181:5791-5802.
9 Gabrilovich DI: Myeloid-derived suppressor cells. Cancer Immunol Res 2017;5:3-8.
10 Gabrilovich DI, Nagaraj S: Myeloid-derived suppressor cells as regulators of the immune system. Nat Rev Immunol 2009;9:162-174.
11 Gorgun GT, Whitehill G, Anderson JL, Hideshima T, Maguire C, Laubach J, Raje N, Munshi NC, Richardson PG, Anderson KC: Tumor-promoting immune-suppressive myeloid-derived suppressor cells in the multiple myeloma microenvironment in humans. Blood 2013;121:2975-2987.
12 Yang L, DeBusk LM, Fukuda K, Fingleton B, Green-Jarvis B, Shyr Y, Matrisian LM, Carbone DP, Lin PC: Expansion of myeloid immune suppressor Gr^+CD11b^+ cells in tumor-bearing host directly promotes tumor angiogenesis. Cancer cell 2004;6:409-421.
13 Liu Y, Lai L, Chen Q, Song Y, Xu S, Ma F, Wang X, Wang J, Yu H, Cao X, Wang Q: MicroRNA-494 is required for the accumulation and functions of tumor-expanded myeloid-derived suppressor cells via targeting of PTEN. J Immunol 2012;188:5500-5510.
14 Li L, Zhang J, Diao W, Wang D, Wei Y, Zhang CY, Zen K: MicroRNA-155 and MicroRNA-21 promote the expansion of functional myeloid-derived suppressor cells. J Immunol 2014;192:1034-1043.
15 Tian J, Rui K, Tang X, Ma J, Wang Y, Tian X, Zhang Y, Xu H, Lu L, Wang S: MicroRNA-9 regulates the differentiation and function of myeloid-derived suppressor cells *via* targeting Runx1. J Immunol 2015;195:1301-1311.
16 Mei S, Xin J, Liu Y, Zhang Y, Liang X, Su X, Yan H, Huang Y, Yang R: MicroRNA-200c promotes suppressive potential of myeloid-derived suppressor cells by modulating PTEN and FOG2 expression. PLoS ONE 2015;10:e0135867.
17 Boldin MP, Taganov KD, Rao DS, Yang L, Zhao JL, Kalwani M, Garcia-Flores Y, Luong M, Devrekanli A, Xu J, Sun G, Tay J, Linsley PS, Baltimore D: miR-146a is a significant brake on autoimmunity, myeloproliferation, and cancer in mice. J Exp Med 2011;208:1189-1201.
18 Liu Q, Zhang M, Jiang X, Zhang Z, Dai L, Min S, Wu X, He Q, Liu J, Zhang Y, Zhang Z, Yang R: miR-223 suppresses differentiation of tumor-induced $CD11b^+$ $Gr1^+$ myeloid-derived suppressor cells from bone marrow cells. Int J Cancer 2011;129:2662-2673.
19 Zhang M, Liu Q, Mi S, Liang X, Zhang Z, Su X, Liu J, Chen Y, Wang M, Zhang Y, Guo F, Zhang Z, Yang R: Both miR-17-5p and miR-20a alleviate suppressive potential of myeloid-derived suppressor cells by modulating STAT3 expression. J Immunol 2011;186:4716-4724.
20 Liu C, Yin J, Xue J, Tao Y, Hu W, Zhang H: *In vitro* effects of amino alcohols on *Echinococcus granulos*us. Acta Trop 2018;182:285-290.
21 Collins TJ: ImageJ for microscopy. Biotechniques 2007;43:25-30.
22 Schneider CA, Rasband WS, Eliceiri KW: NIH Image to ImageJ: 25 years of image analysis. Nat Methods 2012;9:671-675.
23 Vlachos IS, Zagganas K, Paraskevopoulou MD, Georgakilas G, Karagkouni D, Vergoulis T, Dalamagas T, Hatzigeorgiou AG: DIANA-miRPath v3.0: deciphering microRNA function with experimental support. Nucleic Acids Res 2015;43:W460-466.
24 Gabrilovich D, Ishida T, Oyama T, Ran S, Kravtsov V, Nadaf S, Carbone DP: Vascular endothelial growth factor inhibits the development of dendritic cells and dramatically affects the differentiation of multiple hematopoietic lineages *in vivo*. Blood 1998;92:4150-4166.
25 Carmeliet P: VEGF as a key mediator of angiogenesis in cancer. Oncology 2005;69 Suppl 3:4-10.
26 Melgar-Lesmes P, Tugues S, Ros J, Fernandez-Varo G, Morales-Ruiz M, Rodes J, Jimenez W: Vascular endothelial growth factor and angiopoietin-2 play a major role in the pathogenesis of vascular leakage in cirrhotic rats. Gut 2009;58:285-292.
27 Murdoch CE, Bachschmid MM, Matsui R: Regulation of neovascularization by S-glutathionylation *via* the Wnt5a/sFlt-1 pathway. Biochem Soc Trans 2014;42:1665-1670.

28 Maynard SE, Min JY, Merchan J, Lim KH, Li J, Mondal S, Libermann TA, Morgan JP, Sellke FW, Stillman IE, Epstein FH, Sukhatme VP, Karumanchi SA: Excess placental soluble fms-like tyrosine kinase 1 (sFlt1) may contribute to endothelial dysfunction, hypertension, and proteinuria in preeclampsia. J Clin Invest 2003;111:649-658.
29 Kendall RL, Thomas KA: Inhibition of vascular endothelial cell growth factor activity by an endogenously encoded soluble receptor. Proc Natl Acad Sci U S A 1993;90:10705-10709.
30 Luangdilok S, Box C, Harrington K, Rhys-Evans P, Eccles S: MAPK and PI3K signalling differentially regulate angiogenic and lymphangiogenic cytokine secretion in squamous cell carcinoma of the head and neck. Eur J Cancer 2011;47:520-529.
31 Lin Y, Mallen-St Clair J, Wang G, Luo J, Palma-Diaz F, Lai C, Elashoff DA, Sharma S, Dubinett SM, St John M: p38 MAPK mediates epithelial-mesenchymal transition by regulating p38IP and Snail in head and neck squamous cell carcinoma. Oral Oncol 2016;60:81-89.
32 Karar J, Maity A: PI3K/AKT/mTOR pathway in angiogenesis. Front Mol Neurosci 2011;4:51.
33 Trikha P, Carson WE 3rd: Signaling pathways involved in MDSC regulation. Biochim Biophys Acta 2014;1846:55-65.
34 Weichhart T, Costantino G, Poglitsch M, Rosner M, Zeyda M, Stuhlmeier KM, Kolbe T, Stulnig TM, Horl WH, Hengstschlager M, Muller M, Saemann MD: The TSC-mTOR signaling pathway regulates the innate inflammatory response. Immunity 2008;29:565-577.
35 Chen W, Ma T, Shen XN, Xia XF, Xu GD, Bai XL, Liang TB: Macrophage-induced tumor angiogenesis is regulated by the TSC2-mTOR pathway. Cancer Res 2012;72:1363-1372.
36 Yang L, Huang J, Ren X, Gorska AE, Chytil A, Aakre M, Carbone DP, Matrisian LM, Richmond A, Lin PC, Moses HL: Abrogation of TGF beta signaling in mammary carcinomas recruits Gr-1^{+}CD11b^{+} myeloid cells that promote metastasis. Cancer cell 2008;13:23-35.
37 Haskell H, Natarajan M, Hecker TP, Ding Q, Stewart J, Jr., Grammer JR, Gladson CL: Focal adhesion kinase is expressed in the angiogenic blood vessels of malignant astrocytic tumors *in vivo* and promotes capillary tube formation of brain microvascular endothelial cells. Clin Cancer Res 2003;9:2157-2165.
38 Zhao X, Guan JL: Focal adhesion kinase and its signaling pathways in cell migration and angiogenesis. Adv Drug Deliv Rev 2011;63:610-615.
39 Angelucci A, Bologna M: Targeting vascular cell migration as a strategy for blocking angiogenesis: the central role of focal adhesion protein tyrosine kinase family. Curr Pharm Des 2007;13:2129-2145.
40 O'Connell RM, Zhao JL, Rao DS: MicroRNA function in myeloid biology. Blood 2011;118:2960-2969.
41 Yan B, Yao J, Liu JY, Li XM, Wang XQ, Li YJ, Tao ZF, Song YC, Chen Q, Jiang Q: lncRNA-MIAT regulates microvascular dysfunction by functioning as a competing endogenous RNA. Circ Res 2015;116:1143-1156.
42 Jiang Q, Shan K, Qun-Wang X, Zhou RM, Yang H, Liu C, Li YJ, Yao J, Li XM, Shen Y, Cheng H, Yuan J, Zhang YY, Yan B: Long non-coding RNA-MIAT promotes neurovascular remodeling in the eye and brain. Oncotarget 2016;7:49688-49698.
43 Li L, Zhu L, Wang Y, Zhou, Zhu J, Xie W, Ye X: Profiling of microRNAs in AML cells following overexpression or silencing of the VEGF gene. Oncol Lett 2017;13:105-110.
44 Yin R, Wang R, Guo L, Zhang W, Lu Y: MiR-17-3p inhibits angiogenesis by downregulating flk-1 in the cell growth signal pathway. J Vasc Res 2013;50:157-166.
45 Li Y, Kuscu C, Banach A, Zhang Q, Pulkoski-Gross A, Kim D, Liu J, Roth E, Li E, Shroyer KR, Denoya PI, Zhu X, Chen L, Cao J: miR-181a-5p inhibits cancer cell migration and angiogenesis *via* downregulation of matrix metalloproteinase-14. Cancer Res 2015;75:2674-2685.
46 Wang Y, Sun B, Sun H, Zhao X, Wang X, Zhao N, Zhang Y, Li Y, Gu Q, Liu F, Shao B, An J: Regulation of proliferation, angiogenesis and apoptosis in hepatocellular carcinoma by miR-26b-5p. Tumour Biol 2016;37:10965-10979.
47 Lalwani MK, Sharma M, Singh AR, Chauhan RK, Patowary A, Singh N, Scaria V, Sivasubbu S: Reverse genetics screen in zebrafish identifies a role of miR-142a-3p in vascular development and integrity. PLoS ONE 2012;7:e52588.
48 Ma Y, Huang YX, Chen YY: miRNA-34a-5p downregulation of VEGFA in endometrial stem cells contributes to the pathogenesis of endometriosis. Mol Med Rep 2017;16:8259-8264.
49 Miyamoto K, Seki N, Matsushita R, Yonemori M, Yoshino H, Nakagawa M, Enokida H: Tumour-suppressive miRNA-26a-5p and miR-26b-5p inhibit cell aggressiveness by regulating PLOD2 in bladder cancer. Br J Cancer 2016;115:354-363.

50 Si Y, Zhang H, Ning T, Bai M, Wang Y, Yang H, Wang X, Li J, Ying G, Ba Y: miR-26a/b inhibit tumor growth and angiogenesis by targeting the HGF-VEGF axis in gastric carcinoma. Cell Physiol Biochem 2017;42:1670-1683.

51 Chai ZT, Kong J, Zhu XD, Zhang YY, Lu L, Zhou JM, Wang LR, Zhang KZ, Zhang QB, Ao JY, Wang M, Wu WZ, Wang L, Tang ZY, Sun HC: MicroRNA-26a inhibits angiogenesis by down-regulating VEGFA through the PIK3C2α/Akt/HIF-1α pathway in hepatocellular carcinoma. PLoS ONE 2013;8:e77957.

52 Ding L, Ni J, Yang F, Huang L, Deng H, Wu Y, Ding X, Tang J: Promising therapeutic role of miR-27b in tumor. Tumour Biol 2017;39:1010428317691657.